Supporting Information

Di- and Mononuclear Iron Complexes of N,C,S-Tridentate Ligands Containing an Aminopyridyl Group: Effect of the Pendant Amine Site on Catalytic Properties for Proton Reduction

Toyotaka Nakae,[†] Masakazu Hirotsu,*[,†] and Isamu Kinoshita[†,‡]

[†]Graduate School of Science and [‡]The OCU Advanced Research Institute for Natural Science and Technology (OCARINA), Osaka City University, Sumiyoshi-ku, Osaka 558-8585, Japan

E-mail: mhiro@sci.osaka-cu.ac.jp

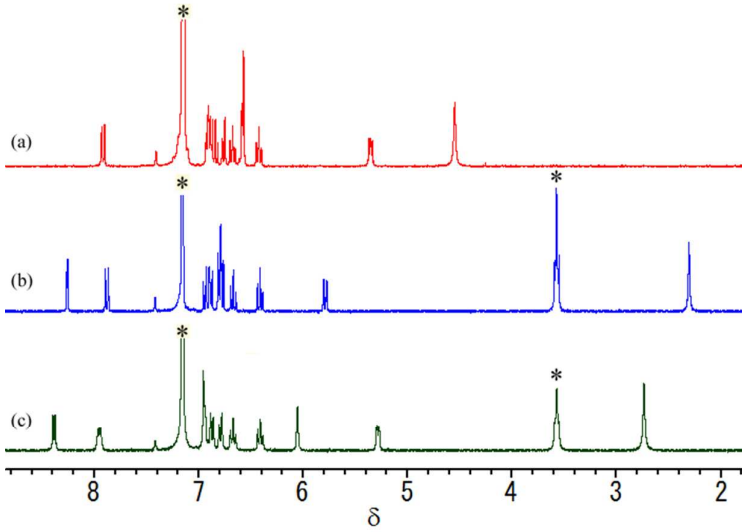

Figure S1. ^{1}H NMR (300 MHz, C_6D_6) spectra of (a) **2**, (b) **3**, and (c) **4**. Residual solvent signals are marked with an asterisk.

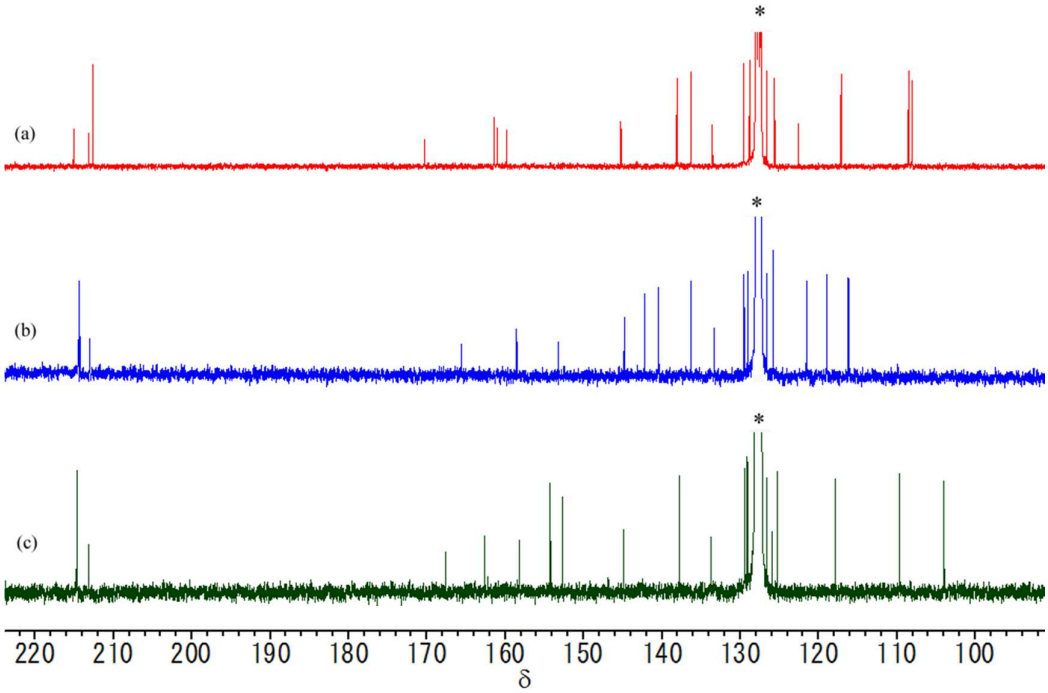

Figure S2. ^{13}C{^{1}H} NMR (75.5 MHz, C_6D_6) spectra of (a) **2**, (b) **3**, and (c) **4**. Residual solvent signals are marked with an asterisk.

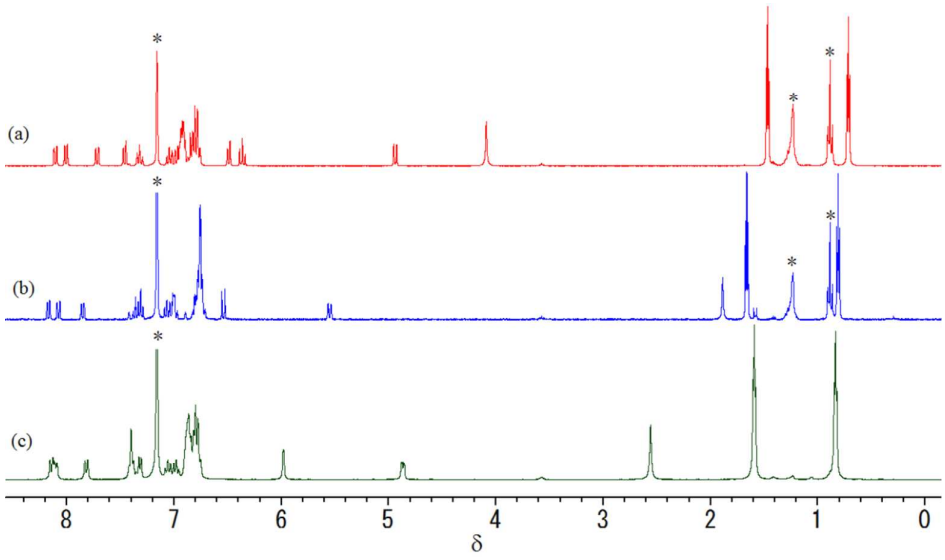

Figure S3. ^{1}H NMR (300 MHz, C_6D_6) spectra of (a) **6**, (b) **7**, and (c) **8**. Residual solvent signals are marked with an asterisk.

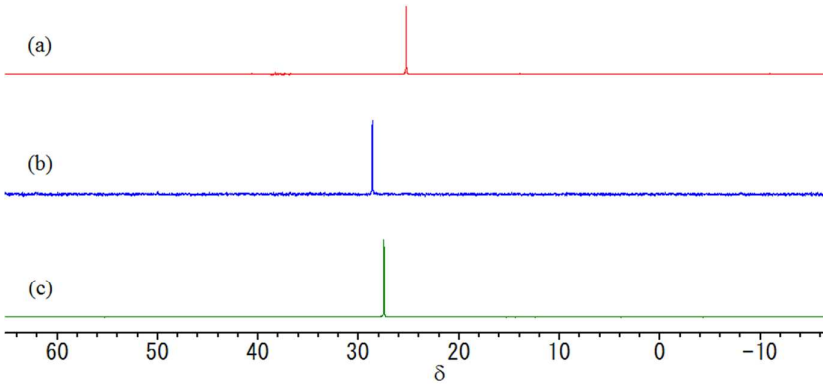

Figure S4. $^{31}P\{^{1}H\}$ NMR (121.5 MHz, C_6D_6) spectra of (a) **6**, (b) **7**, and (c) **8**.

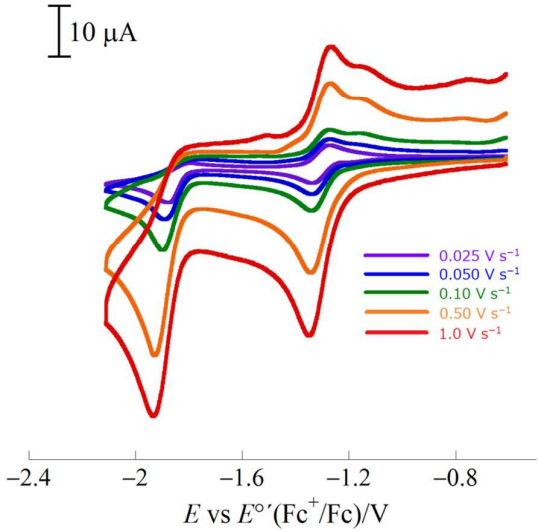

Figure S5. Cyclic voltammograms of **2** (0.5 mM) at a glassy carbon working electrode in CH_3CN containing 0.10 M Bu_4NPF_6 with scan rates from 0.025 to 1 V s^{-1}.

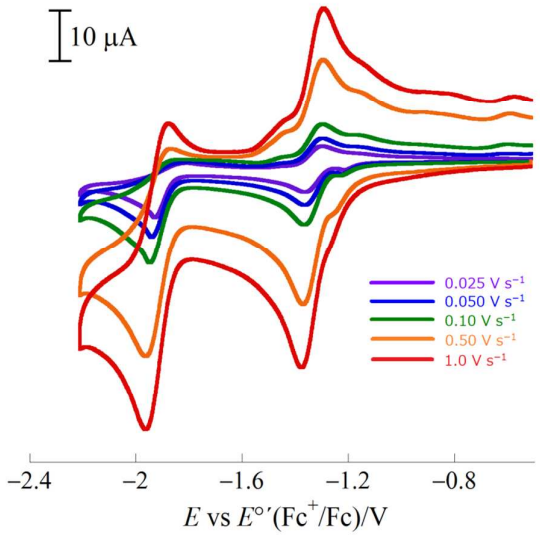

Figure S6. Cyclic voltammograms of **3** in CH_3CN containing 0.10 M Bu_4NPF_6 with scan rates from 0.025 to 1 V s^{-1}.

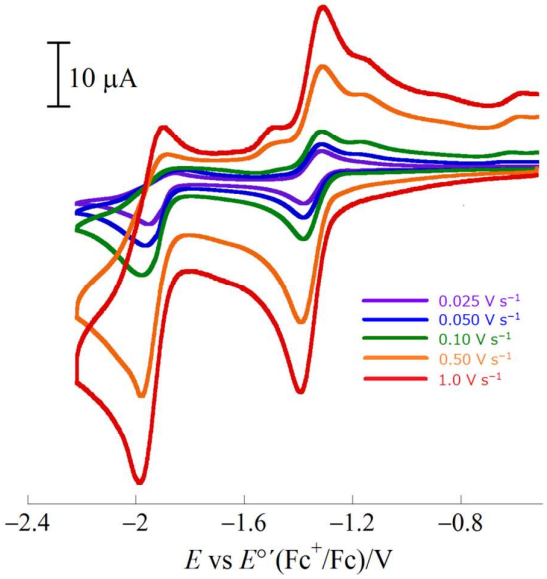

Figure S7. Cyclic voltammograms of **4** (0.5 mM) at a glassy carbon working electrode in CH_3CN containing 0.10 M Bu_4NPF_6 with scan rates from 0.025 to 1 V s^{-1}.

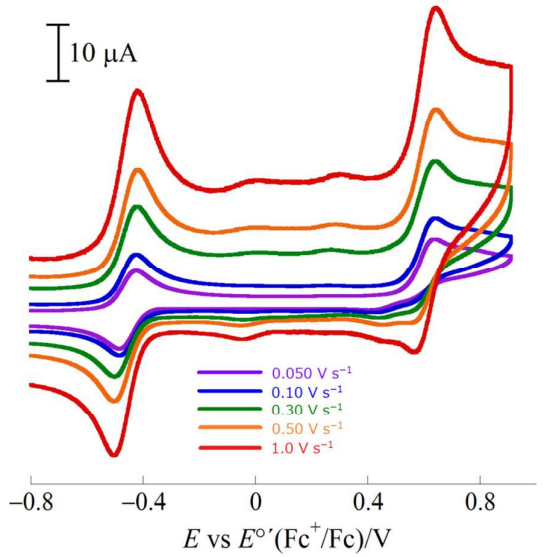

Figure S8. Cyclic voltammograms of **6** (0.5 mM) at a glassy carbon working electrode in CH_3CN containing 0.10 M Bu_4NPF_6 with scan rates from 0.05 to 1 V s^{-1}.

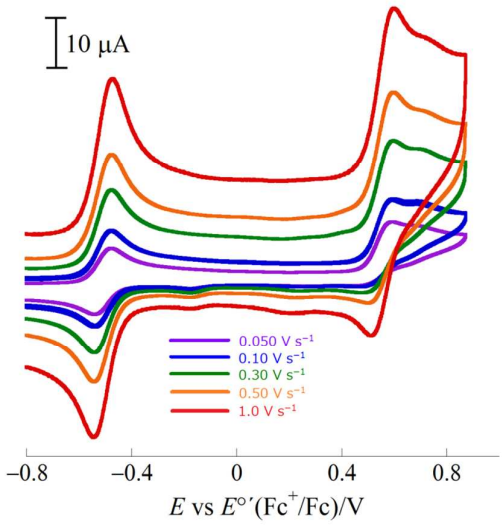

Figure S9. Cyclic voltammograms of **7** (0.5 mM) at a glassy carbon working electrode in CH_3CN containing 0.10 M Bu_4NPF_6 with scan rates from 0.05 to 1 V s^{-1}.

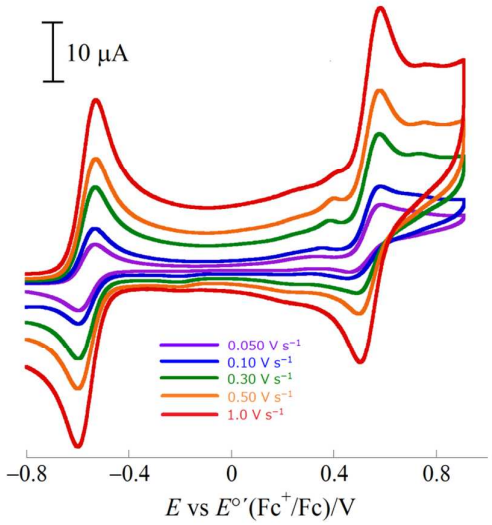

Figure S10. Cyclic voltammograms of **8** (0.5 mM) at a glassy carbon working electrode in CH_3CN containing 0.10 M Bu_4NPF_6 with scan rates from 0.05 to 1 V s^{-1}.

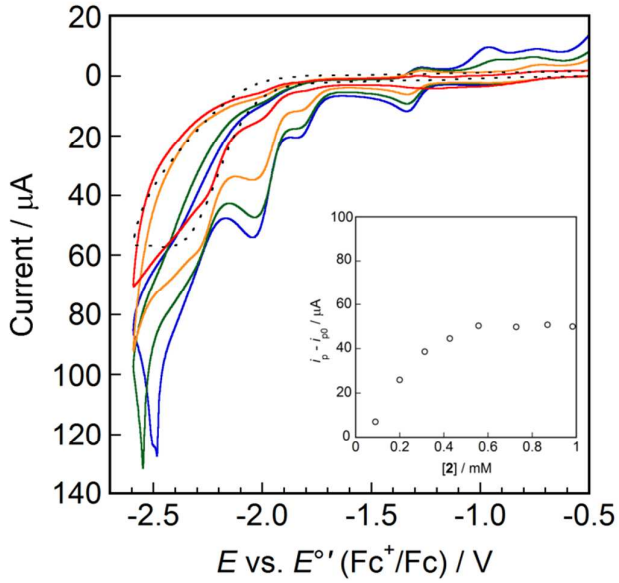

Figure S11. Cyclic voltammograms of acetic acid (5.0 mM) in the presence of **2** in CH_3CN containing 0.10 M Bu_4NPF_6. Concentration of **2**: 0 mM (dotted), 0.089 mM (red), 0.20 mM (orange), 0.31 mM (green), 0.42 mM (blue). Inset: plots of the catalytic peak current measured from current in the absence of **2**.

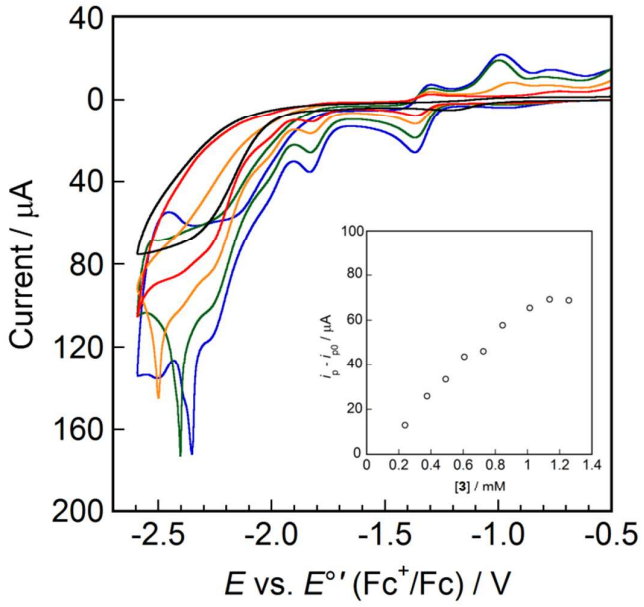

Figure S12. Cyclic voltammograms of acetic acid (5.0 mM) in the presence of **3** in CH_3CN containing 0.10 M Bu_4NPF_6. Concentration of **3**: 0 mM (dotted), 0.24 mM (red), 0.37 mM (orange), 0.49 mM (green), 0.84 mM (blue). Inset: plots of the catalytic peak current measured from current in the absence of **3**.

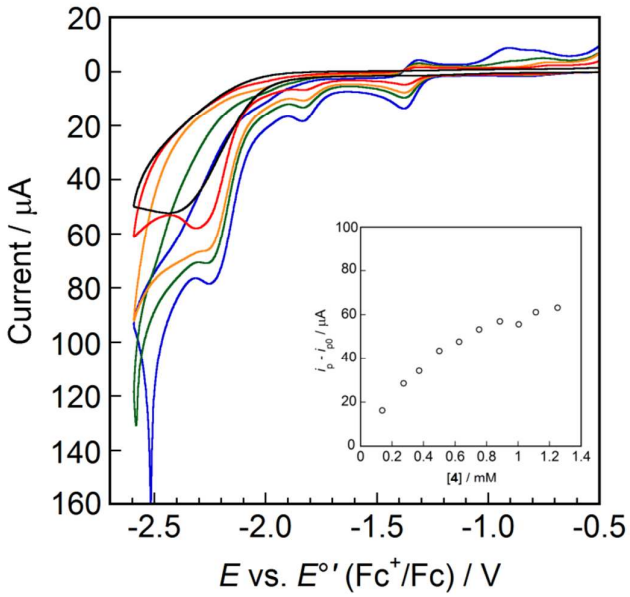

Figure S13. Cyclic voltammograms of acetic acid (5.0 mM) in the presence of **4** in CH_3CN containing 0.10 M Bu_4NPF_6. Concentration of **4**: 0 mM (dotted), 0.14 mM (red), 0.27 mM (orange), 0.37 mM (green), 0.50 mM (blue). Inset: plots of the catalytic peak current measured from current in the absence of **4**.

Table S1. Crystallographic Data for **2** and **3**

	2	**3**
Empirical formula	$C_{22}H_{12}Fe_2N_2O_5S \cdot 1.5(C_4H_8O)$	$C_{22}H_{12}Fe_2N_2O_5S$
Formula weight	636.25	528.10
Temperature/K	133	153
Wavelength/Å	0.71075	0.71075
Crystal system	monoclinic	monoclinic
Space group	*C*2/*c* (No. 15)	$P2_1/c$ (No. 14)
a/Å	32.002(9)	8.9864(18)
b/Å	9.214(2)	13.923(3)
c/Å	21.695(6)	16.560(4)
α/°	90	90
β/°	121.844(3)	103.214(3)
γ/°	90	90
V/Å^3	5434(2)	2017.1(8)
Z	8	4
D_{calcd}/Mg·m^{-3}	1.555	1.739
μ(Mo Kα)/mm^{-1}	1.192	1.581
F(000)	2608	1064.00
Crystal size/mm^3	0.33 × 0.23 × 0.12	0.16 × 0.12 × 0.10
Reflections collected	21652	16345
Independent reflections	6139 (R_{int} = 0.054)	4611 (R_{int} = 0.035)
Completeness to θ	0.994 (θ = 27.39°)	0.996 (θ = 27.49°)
Max. and min. transmission	0.8701 and 0.6944	0.8579 and 0.7860
No. of data/restraints/parameters	6139/79/447	4611/0/337
Goodness of fit on F^2	1.059	1.036
R indices [$I > 2\sigma(I)$]	R_1 = 0.0475	R_1 = 0.0359
R indices (all data)	wR_2 = 0.1101	wR_2 = 0.0840
Largest diff. peak and hole (e·Å^{-3})	0.811 and −0.401	0.435 and −0.294

Table S2. Crystallographic Data for **6**, **7**, and **8**

	6	**7**	**8**
Empirical formula	$C_{34}H_{34}FeN_2OP_2S$	$C_{34}H_{34}FeN_2OP_2S$	$C_{34}H_{34}FeN_2OP_2S$
Formula weight	636.51	636.51	636.51
Temperature/K	153	153	133
Wavelength/Å	0.71075	0.71075	0.71075
Crystal system	monoclinic	monoclinic	monoclinic
Space group	$P2_1/c$ (No. 14)	$P2_1/n$ (No. 14)	$C2/c$ (No. 15)
a/Å	12.8198(19)	13.764(3)	27.492(7)
b/Å	13.4489(18)	15.811(3)	15.535(3)
c/Å	18.317(3)	14.069(3)	19.897(5)
α/°	90	90	90
β/°	108.301 (2)	101.625(3)	134.224(3)
γ/°	90	90	90
V/Å^3	2998.3(8)	2998.9(11)	6090(2)
Z	4	4	8
D_{calcd}/Mg·m^{-3}	1.410	1.410	1.388
μ(Mo Kα)/mm^{-1}	0.711	0.710	0.700
F(000)	1328.00	1328.00	2656.00
Crystal size/mm^3	0.23 × 0.20 × 0.03	0.38 × 0.20 × 0.03	0.18 × 0.13 × 0.05
Reflections collected	24374	24343	24642
Independent reflections	6844 (R_{int} = 0.029)	6778 (R_{int} = 0.048)	6906 (R_{int} = 0.037)
Completeness to θ	0.996 (θ = 27.48°)	0.987 (θ = 27.47°)	0.987 (θ = 27.48°)
Max. and min. transmission	0.9790 and 0.8536	0.9790 and 0.7741	0.9625 and 0.8844
No. of data/restraints/parameters	6844/0/486	6778/0/506	6906/0/506
Goodness of fit on F^2	1.067	1.095	1.074
R indices [$I > 2\sigma(I)$]	R_1 = 0.0385	R_1 = 0.0491	R_1 = 0.0486
R indices (all data)	wR_2 = 0.1009	wR_2 = 0.1039	wR_2 = 0.1169
Largest diff. peak and hole (e·Å^{-3})	0.725 and −0.360	0.334 and −0.351	1.392 and −0.386

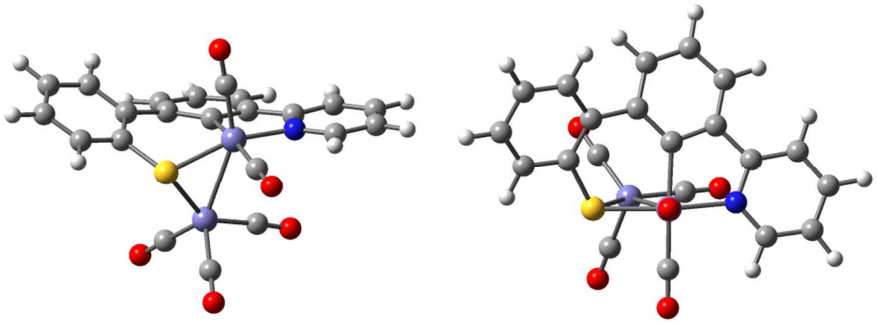

Figure S14. Molecular structures of $\mathbf{1}^{-}$ optimized by the DFT calculation at the B3LYP/6-311+G(d,p) level.

α		β	
LUMO+3 (1.823 eV)		LUMO+4 (1.820 eV)	
LUMO+2 (1.704 eV)		LUMO+3 (1.570 eV)	
LUMO+1 (1.234 eV)		LUMO+2 (1.395 eV)	
LUMO (0.801 eV)		LUMO+1 (1.201 eV)	

HOMO (−2.018 eV)	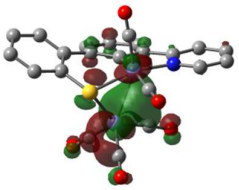	LUMO (0.883 eV)	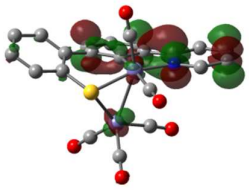
HOMO–1 (−2.469 eV)	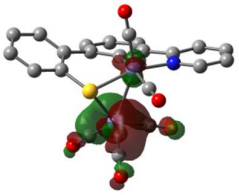	HOMO (−1.735 eV)	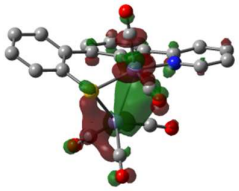
HOMO–2 (−2.729 eV)	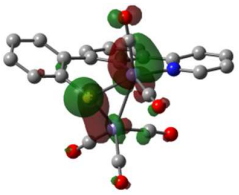	HOMO–1 (−2.450 eV)	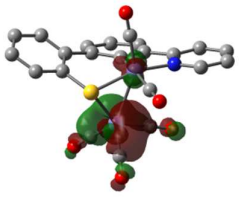
HOMO–3 (−3.057 eV)	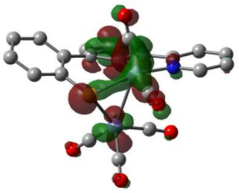	HOMO–2 (−2.803 eV)	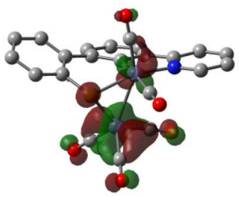
HOMO–4 (−3.172 eV)	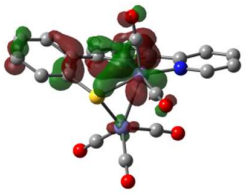	HOMO–3 (−2.866 eV)	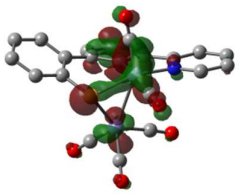
HOMO–5 (−3.343 eV)	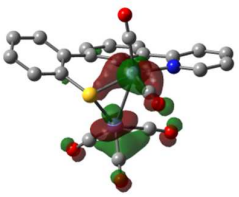	HOMO–4 (−2.989 eV)	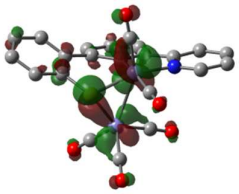

Figure S15. Selected molecular orbitals (isovalue = 0.04) of $\mathbf{1}^{-}$ calculated by DFT at the B3LYP/6-311+G(d,p) level.

Table S3. Molecular Coordinates of $\mathbf{1}^{-}$ Optimized by the DFT Calculation at the B3LYP/6-311+G(d,p) Level

	Atomic number	*x*/Å	*y*/Å	*z*/Å
1	8	2.435927	1.264052	2.195944
2	8	0.033641	4.689022	0.57482
3	6	-0.05208	3.543744	0.701286
4	6	1.416304	1.415414	1.667115
5	8	1.551327	2.447613	-2.60264
6	8	-1.93454	1.676741	3.313059
7	6	-1.2639	1.686216	2.371661
8	26	-0.17957	1.724937	0.916608
9	16	-1.44282	1.157629	-0.92172
10	6	1.16039	1.539761	-2.00555
11	26	0.550273	0.088054	-1.11648
12	6	-2.73137	-0.04973	-0.65513
13	6	-3.98441	0.295164	-1.18417
14	6	3.553728	-0.15582	-1.15244
15	7	2.389385	-0.56952	-0.61461
16	6	4.785466	-0.68219	-0.8079
17	6	0.001239	-1.30083	0.211195
18	6	-1.28831	-1.726	0.635671
19	6	-2.54942	-1.30091	-0.0287
20	6	-5.05944	-0.58284	-1.14152
21	6	2.421317	-1.56123	0.319823
22	6	-1.40948	-2.60317	1.727839
23	6	1.112423	-1.93923	0.835498
24	6	4.829733	-1.70506	0.143856
25	6	0.236276	-0.96364	-2.51055
26	6	3.642813	-2.14191	0.7016
27	6	-0.29963	-3.15911	2.359427
28	6	-3.64501	-2.18872	-0.04446
29	6	0.967294	-2.85077	1.890649
30	6	-4.87945	-1.84698	-0.58147
31	8	-0.0053	-1.64335	-3.41313
32	1	3.48434	0.632853	-1.8896
33	1	5.683459	-0.29747	-1.27537
34	1	5.773984	-2.14843	0.440576
35	1	3.647583	-2.9362	1.435916
36	1	1.834387	-3.29504	2.367917

37	1	-0.42936	-3.81969	3.209999
38	1	-2.39479	-2.83846	2.113917
39	1	-3.51146	-3.18568	0.357723
40	1	-5.69022	-2.56818	-0.57377
41	1	-6.01668	-0.29258	-1.56203
42	1	-4.0954	1.26999	-1.64582

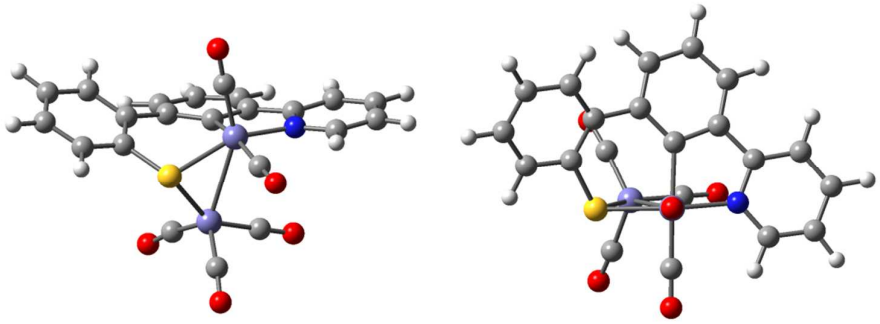

Figure S16. Molecular structures of $\mathbf{1}^{2-}$ optimized by the DFT calculation at the B3LYP/6-311+G(d,p) level.

LUMO+3 (4.308 eV)	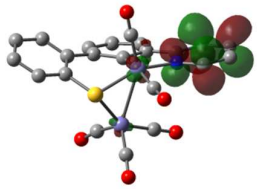	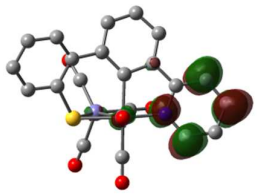
LUMO+2 (4.160 eV)	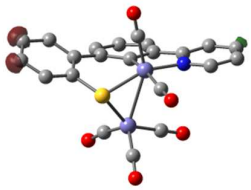	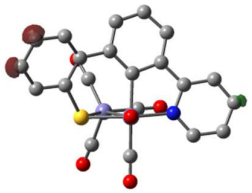
LUMO+1 (3.938 eV)	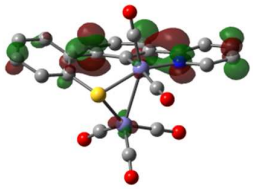	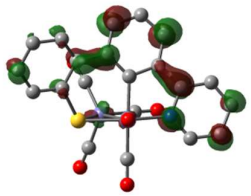
LUMO (3.928 eV)	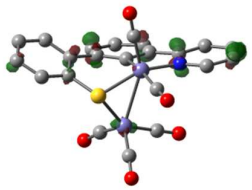	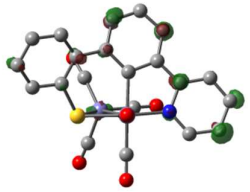

HOMO (2.076 eV)	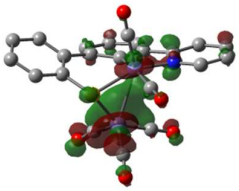	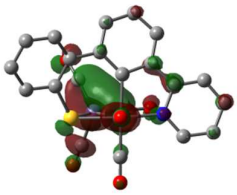
HOMO–1 (1.717 eV)	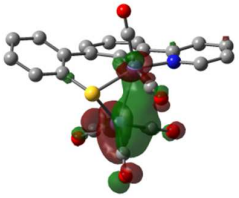	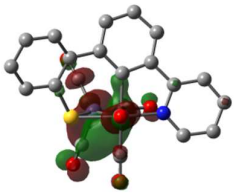
HOMO–2 (0.912 eV)	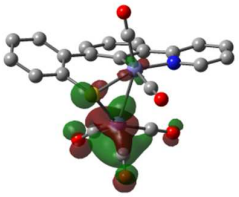	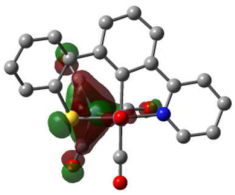
HOMO–3 (0.598 eV)	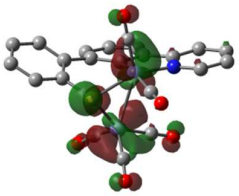	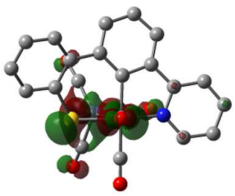
HOMO–4 (0.349 eV)	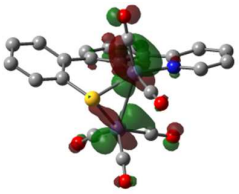	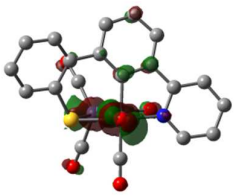
HOMO–5 (0.072 eV)	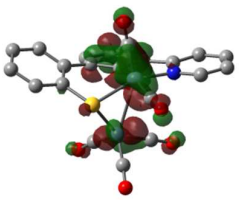	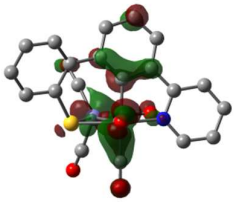

Figure S17. Selected molecular orbitals (isovalue = 0.04) of $\mathbf{1}^{2-}$ calculated by DFT at the B3LYP/6-311+G(d,p) level.

Table S4. Molecular Coordinates of $\mathbf{1}^{2-}$ Optimized by the DFT Calculation at the B3LYP/6-311+G(d,p) Level

	Atomic number	*x*/Å	*y*/Å	*z*/Å
1	8	2.41265	1.360227	2.325588
2	8	0.07377	4.656987	0.740956
3	6	0.001827	3.483644	0.726794
4	6	1.384639	1.520529	1.793833
5	8	1.588019	2.48898	-2.5261
6	8	-1.81358	1.138693	3.321924
7	6	-1.15845	1.286801	2.35985
8	26	-0.15704	1.750731	0.989067
9	16	-1.40662	1.254327	-0.83056
10	6	1.17714	1.565957	-1.95194
11	26	0.546729	0.083633	-1.14375
12	6	-2.71839	0.049724	-0.62467
13	6	-3.96888	0.436176	-1.13271
14	6	3.535982	-0.13939	-1.14797
15	7	2.355638	-0.55504	-0.62765
16	6	4.759616	-0.69978	-0.84474
17	6	-0.00911	-1.28	0.175613
18	6	-1.31075	-1.71819	0.58545
19	6	-2.56393	-1.2354	-0.05447
20	6	-5.06486	-0.41943	-1.13004
21	6	2.391633	-1.60799	0.262996
22	6	-1.44817	-2.64614	1.623829
23	6	1.093964	-1.98665	0.762767
24	6	4.804779	-1.78177	0.055382
25	6	0.175568	-0.8711	-2.55455
26	6	3.612936	-2.2232	0.59696
27	6	-0.34194	-3.25366	2.233535
28	6	-3.67724	-2.09978	-0.11376
29	6	0.92644	-2.94445	1.779717
30	6	-4.90901	-1.71222	-0.63022
31	8	-0.04406	-1.50236	-3.51191
32	1	3.477921	0.691751	-1.83853
33	1	5.658399	-0.29531	-1.29725
34	1	5.745818	-2.25399	0.319778
35	1	3.607057	-3.05652	1.289278
36	1	1.788513	-3.42305	2.23651

37	1	-0.48483	-3.94882	3.055915
38	1	-2.43735	-2.88171	2.002442
39	1	-3.5589	-3.11759	0.240047
40	1	-5.73337	-2.41981	-0.65433
41	1	-6.01763	-0.08959	-1.53549
42	1	-4.05832	1.434815	-1.54788

Table S5. Charge Distributions Calculated by Natural Population Analysis for **1**,[a] $\mathbf{1}^{-}$, and $\mathbf{1}^{2-}$

Basis set	6-311G(d,p) [b]			6-311+G(d,p)		
Complex	**1**[a]	$\mathbf{1}^{-}$	$\mathbf{1}^{2-}$	**1**[a]	$\mathbf{1}^{-}$	$\mathbf{1}^{2-}$
Fe1[c]	0.639	0.574	0.562	−0.090	−1.238	−1.277
Fe2[c]	0.474	0.560	0.348	−0.287	−1.214	−1.567
PyBPT[d]	−0.707	−0.994	−1.409	−0.281	0.093	−0.242
$(CO)_5$[d]	−0.406	−1.140	−1.502	0.658	1.360	1.085
Δ(Fe1−Fe2)[e]	0.165	0.014	0.214	0.197	−0.024	0.290

[a] Data from ref 1. [b] Structures optimized at the B3LYP/6-311+G(d,p) level were used. [c] Fe1 is in the $Fe(PyBPT)(CO)_2$ unit, and Fe2 is in the $Fe(CO)_3$ unit. [d] Sum of the atomic charges on the ligand. [e] Differences in atomic charge between Fe1 and Fe2.

Reference

(1) Hirotsu, M.; Santo, K.; Tsuboi, C.; Kinoshita, I. *Organometallics* **2014**, *33*, 4260–4268.